Available online at www.sciencedirect.com
SCIENCE DIRECT®
Journal of Magnetic Resonance 162 (2003) 454–465
JMR Journal of Magnetic Resonance
www.elsevier.com/locate/jmr

High frequency and field EPR spectroscopy of Mn(III) complexes in frozen solutions

J. Krzystek[a,*] and Joshua Telser[b]

[a] *Center for Interdisciplinary Magnetic Resonance, National High Magnetic Field Laboratory, Florida State University, 1800 E. Paul Dirac Drive, Tallahassee, FL 32310, USA*
[b] *Chemistry Program, Roosevelt University, Chicago, IL 60605, USA*

Received 11 November 2002; revised 16 January 2003

Abstract

We have performed high-frequency and -field electron paramagnetic resonance (HFEPR) experiments on two complexes of high-spin Mn(III) ($3d^4, S = 2$): mesotetrasulfonato-porphyrinatomanganese(III) (Mn(TSP)) and [(*R*,*R*)-(−)-*N*,*N*′-bis(3,5-di-*tert*-butylsalicylidene)-1,2-cyclohexanediaminomanganese(III)] (Mn(salen)). The main aim of this work was to qualitatively and quantitatively characterize the conditions suitable for HFEPR of high-spin transition metal complexes in frozen solutions, and compare them with experiments performed on solid samples. Mn(TSP) is a porphyrin complex soluble in water, in contrast to most metalloporphyrins. Mn(salen), often referred to as Jacobsen's catalyst, is a complex widely used in organic synthesis for alkene epoxidation, and is soluble in organic solvents. High-quality HFEPR signals were observed for solid state Mn(TSP), as has been previously shown for many Mn(III) complexes. The present study is, however, the first to report high-quality HFEPR spectra of a Mn(III) complex in frozen aqueous solution. Analysis of the data yielded the following spin Hamiltonian parameters: $S = 2$; $D = -3.16 \pm 0.02\,\mathrm{cm}^{-1}$, $E = 0$, and isotropic $g = 2.00(2)$. No X-band EPR signals were observed for Mn(TSP), which is a consequence of this being a rigorously axial spin system. Mn(salen), in contrast, did not give good quality HFEPR spectra in the solid state, but high-quality HFEPR spectra were recorded in frozen organic solutions. Analysis of the data yielded the following spin Hamiltonian parameters: $S = 2$; $D = -2.47 \pm 0.02\,\mathrm{cm}^{-1}$, $|E| = 0.17 \pm 0.01\,\mathrm{cm}^{-1}$, and isotropic $g = 2.00(2)$. These values differ from those reported using X-band parallel mode EPR [J. Am. Chem. Soc. 123 (2001) 5710], as discussed in the text. Therefore, a comparison between HFEPR and parallel-mode X-band spectroscopy is made. Finally, the concentration sensitivity aspect of HFEPR spectroscopy is also discussed.

1. Introduction

HFEPR,[1] defined here as: $\nu \geqslant 94\,\mathrm{GHz}$, $0 \leqslant B_0 \leqslant 25\,\mathrm{T}$, has been very successful in recent years in detecting and characterizing EPR signals from a variety of integer spin (non-Kramers) transition metal complexes [1,2]. These complexes had been traditionally dubbed 'EPR-silent' due to their typically large zfs and lack of a doubly degenerate $M_S = \pm 1/2$ Kramers doublet [3]. They included such transition metal ions as Cr(II) [4], Fe(II) [5], V(III) [6], Ni(II) [7], and particularly Mn(III) [8–13]. The number of publications describing various Mn(III) complexes underscores the importance of high-spin ($S = 2$) Mn(III) in its role as a building block in molecular magnets [14–22], as a catalyst for organic reactions [23–25], and also in biochemical reaction cycles [26–28].

A vast majority of the HFEPR experiments performed on molecular Mn(III) complexes, and indeed on all non-Kramers ion complexes, was done on solid samples (a single study [4] dealt with a molecular complex of high-spin non-Kramers metal ion in solution: $[Cr(H_2O)_6]^{2+}$). It is quite appropriate to investigate by

* Corresponding author. Fax: 1-850-644-9462.
E-mail address: krzystek@magnet.fsu.edu (J. Krzystek).

[1] *Abbreviations used:* EPR, Electron paramagnetic resonance; HFEPR: high frequency and field EPR; hfs: hyperfine structure; Mn(TSP): mesotetrasulfonato-porphyrinatomanganese(III); Mn(salen): [(*R*,*R*)-(−)-*N*,*N*′-bis(3,5-di-*tert*-butylsalicylidene)-1,2-cyclohexanediaminomanganese(III); Mn(TPP): tetraphenylporphyrinatomanganese(III); NMO: *N*-methylmorpholine *N*-oxide; *S*/*N*: signal-to-noise; zfs: zero-field splitting.

1090-7807/03/$ - see front matter © 2003 Elsevier Science (USA). All rights reserved.
doi:10.1016/S1090-7807(03)00042-9

HFEPR molecular complexes of Mn(III) or other transition metal ions with magnetic and/or heterogeneous catalytic properties in the solid state. However, for systems with biological relevance or homogeneous catalytic properties, solutions are far preferable. Only the most recent work reported from this laboratory [11,29,30] made inroads into HFEPR of frozen organic solutions of certain molecular Mn(III) complexes. The main reason for this scarcity of data lies in the inherent experimental difficulties associated with performing HFEPR experiments on high-spin species in solution, some of which were recognized in the review by Hagen [1]. These concern the minimal *concentration* sensitivity (as opposed to absolute sensitivity) of the HFEPR spectrometers, and the high dielectric losses caused by most solvents at millimeter and sub-millimeter wavelengths. It is therefore the principal goal of this work to discuss in a systematic way the problems encountered while employing HFEPR to study high-spin non-Kramers ions in frozen solutions, based on two high-spin Mn(III) complexes: Mn(TSP) [31], and Mn(salen) [32] (Scheme 1). The results of HFEPR experiments on frozen solutions of both complexes were compared with those obtained from solid samples.

The two Mn(III) complexes were chosen for several reasons: Mn(TSP) is representative of the series of Mn(III) tetrapyrrole complexes [30] characterized by Mn(III) in square planar or square pyramidal geometry with rigorously axial molecular symmetry. In contrast to most porphyrinic complexes, Mn(TSP) is water-soluble, and is thus optimal for investigating experimental conditions in an aqueous frozen solution. Mn(salen) on the other hand is representative of Mn(III) complexes of distorted octahedral geometry (when in the presence of a coordinating solvent) and non-axial (rhombic) molecular symmetry and is soluble only in organic solvents. Mn(salen) is a chiral complex that is of great utility as a catalyst for the enantioselective epoxidation of alkenes [24]. It was the Fluka Prize "Reagent of the Year" in 1994 [33]. Neither complex has been studied before by HFEPR to our best knowledge, although Mn(salen) was an object of an excellent X-band EPR study by Campbell et al. [25] using parallel-mode detection. Since the latter technique has been in use for some time to study $S = 2$ species [25,28,34,35], a secondary goal of this work has thus been to compare the two alternative techniques used to study $S = 2$ transition metal complexes: HFEPR and parallel-mode X-band EPR.

The experiments were performed in two different HFEPR spectrometers, both locally-constructed: the transmission-type instrument described previously [36], and the new generation device based on the principles of quasi-optical millimeter and sub-millimeter wave propagation (C. Saylor et al. to be published). An additional goal of the current work was thus to compare the performance of these two basic HFEPR spectrometer designs in investigating non-Kramers transition metal ion complexes generally, and in frozen solutions in particular, in terms of achieved concentration sensitivity.

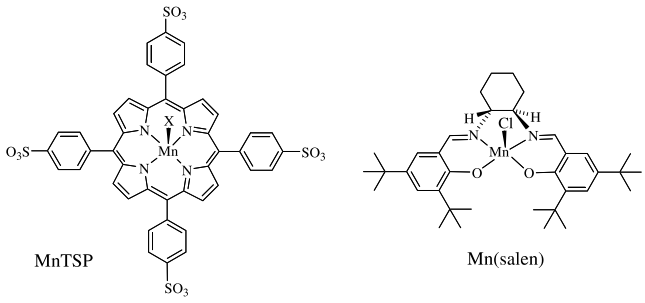

Scheme 1.

2. Experimental

2.1. Materials

Mn(TSP) was purchased from Porphyrin Products, Logan, UT and used as a solid 'as is.' For the purpose of producing a low-temperature glass, the solid was dissolved in doubly distilled water at a concentration of 55 mM. Since adding a glassing agent, e.g. methanol, led to demetallation of the complex, no such agent was employed, nor was any buffering medium used. The solution was purged with nitrogen before freezing to reduce dissolved oxygen concentration. Mn(salen) was purchased from Aldrich–Sigma and used as a solid 'as is.' Alternatively, it was ground and embedded in *n*-eicosane (Aldrich–Sigma, $C_{20}H_{42}$, mp 37 °C), or in a KBr pellet. For producing a low-temperature glass the material was dissolved in methylene chloride (CH_2Cl_2), and subsequently toluene (both from Aldrich–Sigma, spectroscopy grade) was added to achieve a proportion of 3:2 CH_2Cl_2:toluene v/v. The solvents had been thoroughly purged with nitrogen to reduce dissolved oxygen concentration. The final concentration of Mn(salen) was about 200 mM. NMO (Aldrich–Sigma, analytical grade) was used 'as is.'

2.2. Instrumentation

Two different locally constructed HFEPR spectrometers were used. The first instrument was a transmission-type device in which the millimeter and sub-millimeter waves are propagated in cylindrical lightpipes, as described previously [36]. Millimeter and sub-millimeter frequencies were generated by either of two Gunn oscillators, operating at 95 ± 3 and 110 ± 3 GHz, respectively. For most applications, and in the sensitivity estimates presented in this work, the frequencies were multiplied by factors of two or three using Schottky diode-based multipliers. The power emitted at the

second harmonic of the basic frequency was about 4 mW, while that emitted at the third harmonic was about 1 mW. The second spectrometer is of a newer generation homodyne design in which the millimeter and sub-millimeter waves are propagated in free space (outside the magnet) using quasi-optical principles, and in a corrugated waveguide within the magnet bore. This method of propagation reduces power transmission losses by about two orders of magnitude, and allows control of the signal phase. This spectrometer is of a homodyne reflection type, and thus follows the design principles described previously [37,38]. It will be presented in more detail in an upcoming paper (C. Saylor et al., to be published). Millimeter and sub-millimeter frequencies were generated by the same Gunn diodes as in the transmission spectrometer, therefore the same power was available at the source. Neither spectrometer used a resonator. Temperature control was achieved with an Oxford Instruments CF1200 continuous flow liquid helium cryostat and an IC503 controller. Field modulation and phase-sensitive detection using a lock-in amplifier was employed.

2.3. Computer software

The program SIM written by Weihe [39,40] was used to generate powder pattern EPR spectra for particular frequencies, allowing direct assignment of the observed EPR transitions. The program is based on a full-matrix diagonalization procedure and is therefore adequate to spin systems with any value of zfs parameters relative to the operating frequency. Our use of the program assumed a colinearity of the $\boldsymbol{g}$ and zfs tensors, as is usually done for high symmetry molecules [41], such as the systems studied here, although in low symmetry molecules, this assumption may not be valid [13], and the program allows for non-colinearity. The program also takes into account the Boltzmann population factor in calculating the transition intensities.

3. Spectra and spectral interpretation

3.1. Mn(TSP)

Unlike most solid Mn(III) porphyrin-like complexes studied so far [9–11,29,30] solid polycrystalline Mn(TSP) does *not* orient in magnetic field. Neither does it show other symptoms often associated with solid samples of high-spin transition metal complexes, such as a 'pseudo-noise' originating from a discrete number of crystallites [42]. HFEPR spectra produced by the polycrystalline solid are therefore almost perfect powder patterns; there is no need to restrain the sample as was necessary with many other Mn(III) and other high-spin transition metal ions [10,11,29,43]. Fig. 1 presents

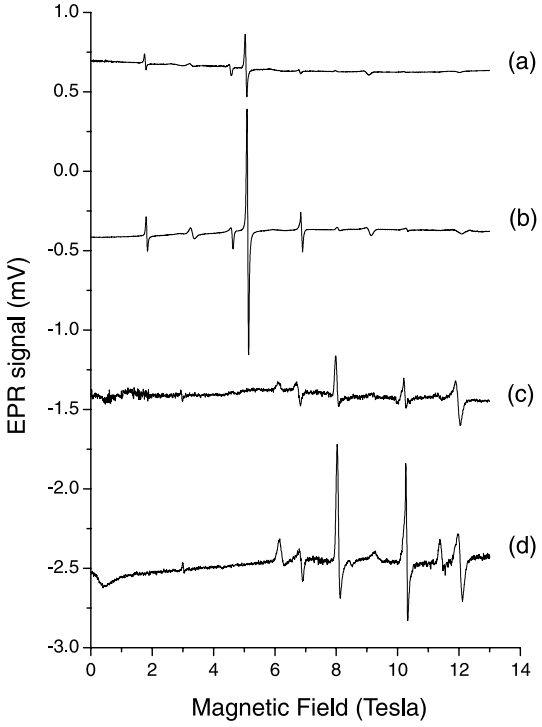

Fig. 1. HFEPR spectra of Mn(TSP) recorded in the transmission-type spectrometer at 20 K. The same mass of sample (14.1 mg) was used in each experiment. (a) Solid polycrystalline sample at 191.52 GHz; (b) frozen solution in water at 191.52 GHz; (c) solid polycrystalline sample at 287.28 GHz; (d) frozen solution in water at 287.28 GHz. The 287 GHz spectra (c and d) are amplified by a factor of 10 with regard to the spectra acquired at 192 GHz (a and b). Otherwise all instrumental settings remained unchanged, except for the millimeter wave power that was strongly frequency-dependent and was smaller by a factor of about 10 at 287 GHz than at 192 GHz: field sweep rate: 0.2 T/min; field modulation: 8 kHz frequency, 1.5 mT amplitude; time constant: 0.3 s.

HFEPR spectra of *solid* polycrystalline Mn(TSP) taken at frequencies of ca. 192 (Fig. 1a), and 287 GHz (Fig. 1c), and temperature of 30 K, in the transmission-type HFEPR spectrometer. Figs. 2a and c shows analogous spectra recorded at the frequencies of ca. 108 and 328 GHz, respectively, at 20 K in the same spectrometer. Spectra could be recorded without noticeable changes in other than signal amplitude from 5 K up to about 50 K.

HFEPR spectra of the low-temperature *aqueous solutions* of Mn(TSP) at a concentration of 55 mM are shown in Figs. 1b and d in the same spectrometer and in experimental conditions identical to Figs. 1a and c, respectively. The solution volume (250 μL) was carefully chosen so that the mass of Mn(TSP) (14.1 mg) was identical in all four spectra. Fig. 3a shows an HFEPR spectrum of the same 55 mM aqueous solution of Mn(TSP) recorded in the quasi-optical reflection-type HFEPR spectrometer at 220 GHz. Because of the smaller sample volume in this spectrometer (40 μL), the mass of Mn(TSP) (2.2 mg) was correspondingly smaller in this experiment than in the transmission apparatus.

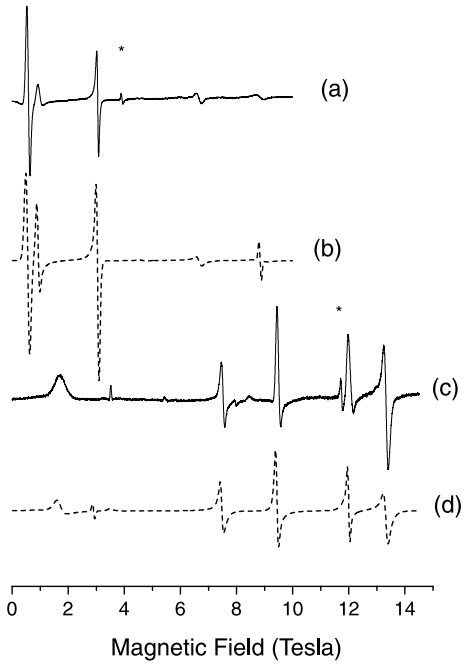

Fig. 2. HFEPR spectra of solid polycrystalline Mn(TSP) recorded in the transmission-type spectrometer at 20 K. (a) Experiment at the frequency of 108.38 GHz; (b) simulation at same frequency using the following spin Hamiltonian parameters: $D = -3.12\,\mathrm{cm}^{-1}$, $E = 0$, $g(\mathrm{iso}) = 2.00$, single-crystal linewidth 100 mT (parallel transitions), 50 mT (perpendicular transitions); (c) frequency of 328.16 GHz; (d) simulation at same frequency using the same set of spin Hamiltonian parameters as in (b). Instrumental settings are identical to Fig. 1. The incident millimeter or sub-millimeter wave power is strongly frequency-dependent. Signals marked with asterisk (*) originate from a high-symmetry Mn(II) impurity and are therefore not reproduced in the simulations.

A comparison of Figs. 1a, b and 1c, d, respectively, shows that the spectra recorded at a given frequency from a solid sample, and from a frozen aqueous solution were identical with respect to spectral features. This proves beyond doubt that solid polycrystalline Mn(TSP) does not undergo the torquing effect in magnetic field. The amplitudes of the solution spectra were consistently higher by a factor of 3–5 than those of the solid sample for the same mass of Mn(TSP). No hyperfine structure due to the $I = 5/2$ nuclear spin of ^{55}Mn was observed in any experimental conditions, including diluting the sample to the detection limit.

To analyze the obtained spectra, we applied the standard spin Hamiltonian for the quintet ($S = 2$) spin state, in which are included second order zfs terms D and E, and fourth order zfs terms a (cubic) and F (axial) [3]:

$$\begin{aligned}\mathcal{H} = {} & \beta B\cdot\mathbf{g}\cdot S + D[S_z^2 - S(S+1)/3] + E(S_x^2 - S_y^2) \\ & + (a/6)[S_x^4 + S_y^4 + S_z^4 - (1/5)S(S+1)(3S^2 \\ & + 3S - 1)] + (F/180)[35S_z^4 - 30S(S+1)S_z^2 \\ & + 25S_z^2 - 6S(S+1) + 3S^2(S+1)]. \qquad (1)\end{aligned}$$

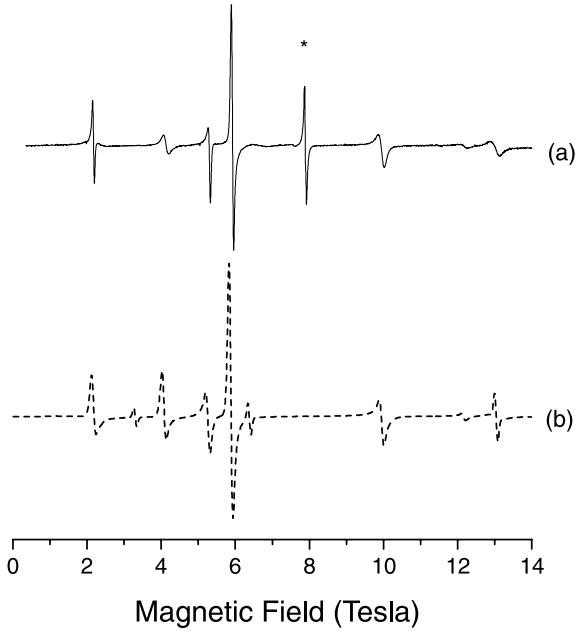

Fig. 3. (a) HFEPR spectrum of a 55 mM Mn(TSP) solution in water at 220.05 GHz recorded in the quasi-optical reflection-type spectrometer at 30 K. Field sweep rate: 0.5 T/min; field modulation: 20 kHz frequency, 0.75 mT amplitude; time constant: 0.3 s; (b) simulation generated for the same frequency and temperature using the following spin Hamiltonian parameters: $D = -3.17\,\mathrm{cm}^{-1}$, $E = 0$, $g(\mathrm{iso}) = 2.00$, single-crystal linewidth 50 mT (isotropic). Signal marked with asterisk (*) originates from a high-symmetry Mn(II) impurity and exhibits well-resolved hfs under high-resolution conditions (not shown).

We found that satisfactory agreement between HFEPR spectra and simulations was achieved without the fourth order terms, so that the spin Hamiltonian used for interpretation of HFEPR data became truncated to:

$$\mathcal{H} = \beta B\cdot\mathbf{g}\cdot S + D(S_z^2 - S(S+1)/3) + E(S_x^2 - S_y^2). \qquad (2)$$

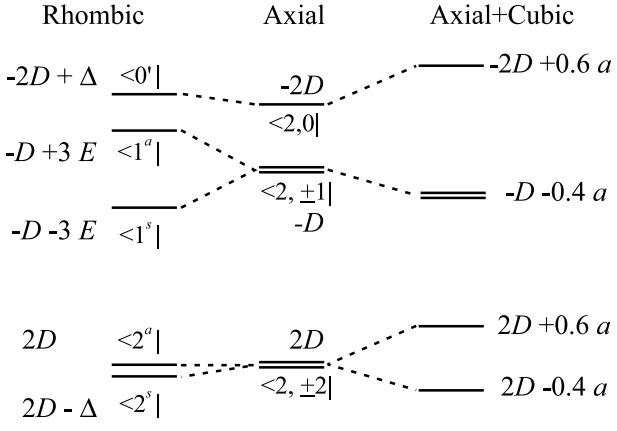

Fig. 4. Effect of Hamiltonian (1) acting on the quintet spin state wavefunctions in zero field. For clarity, no fourth order axial or rhombic terms were included. $\Delta = 3E^2/D$.

However, fourth order terms may be relevant to interpreting X-band data (see Section 4) The effect of Hamiltonian (1) acting on the spin wavefunctions of the quintet spin in zero field is illustrated in Fig. 4.

Because of the lack of the torquing effect, we could not use the approach we applied in our previous studies of solid porphyrinic Mn(III) complexes [9–11,29], namely using the frequency dependence of the quasi-single crystal spectra resulting from that effect to immediately obtain the approximate value of D. Rather, we have used the full diagram of spin sublevels characteristic for $S = 2$ in zero field (Fig. 4). We thus noticed that the 287 GHz spectrum of Mn(TSP) contains a transition at, or near zero field (Fig. 1d). This would correspond to the transition between the zero-field levels characterized by $|S, M_S\rangle = |2, \pm 2\rangle$, and $|2, \pm 1\rangle$, or $|2, \pm 1\rangle$ and $|2, 0\rangle$ (the third possibility, a transition between the $|2, \pm 2\rangle$ and $|2, 0\rangle$ levels is less likely). In the first case, the energy gap between the two levels would correspond to $3|D|$, and would point at a negative D (the $|S, M_S\rangle = |2, \pm 2\rangle$ spin level being the ground level), while in the second case the energy gap would be equal to $|D|$, and would point at positive D (the $|S, M_S\rangle = |2, 0\rangle$ spin level being the ground level). By analogy with previously studied porphyrinic complexes of Mn(III) we assumed the first case to be true, and thus obtained an estimate for $D = -3.15\,\mathrm{cm}^{-1}$. We also assumed an axial spin Hamiltonian, i.e. $E = 0$, by analogy with all other porphyrinic Mn(III) complexes studied so far [44].

We then proceeded to simulate individual spectra recorded at different frequencies. Figs. 2b and d contain simulated spectra for solid Mn(TSP) at 108 and 328 GHz next to the experimental spectra taken at the same frequencies, while Fig. 3b contains an analogous simulated spectrum at 220 GHz placed next to the experimental spectrum recorded for the frozen solution at the same frequency. The simulations yielded the best agreement with the experiment on the solid using $D = -3.12 \pm 0.02\,\mathrm{cm}^{-1}$, $E = 0$, and isotropic $g = 2.00(2)$. No measurable rhombicity of the zfs tensor could be observed, and the anisotropy of the g tensor was also within experimental error. For the aqueous solution spectra of Mn(TSP), the best-fit spin Hamiltonian parameters obtained by single-frequency simulations were $D = -3.16 \pm 0.02\,\mathrm{cm}^{-1}$, $E = 0$, and isotropic $g = 2.00(2)$. Our criterion of a 'good' fit was that no line in the simulated spectrum differed from the experiment by more than half the linewidth.

For comparison, an X-band EPR experiment on a frozen solution sample of Mn(TSP) at 20 K was performed in the laboratory of Professor R.D. Britt, using parallel-mode detection [25]. No signals could be observed under these conditions.

3.2. Mn(salen)

In contrast to Mn(TSP), solid polycrystalline Mn(salen) *does* orient in field, similarly to many other Mn(III) complexes. At low temperature (5.0 K) a single line was observed in fields significantly lower than those corresponding to the $g = 2$ condition (inset in Fig. 5). We have identified this line with the parallel $|S, M_S\rangle = |2, -2\rangle \rightarrow |2, -1\rangle$ transition, analogously to other Mn(III) complexes [9,10,29]. The procedure outlined previously [9] was subsequently applied, namely collecting spectra at several frequencies, and estimating the zfs parameter D from the obtained dependency (Fig. 5) with the caveat that this procedure is best only for systems of axial, or near-axial symmetry of the zfs tensor. Given the reported small rhombicity of the Mn(salen) zfs tensor [25], this procedure is justified since it introduces an error on the order of 1% of the D value only. From the plot presented in Fig. 5, we obtained $D = -2.24\,\mathrm{cm}^{-1}$ and $g_z = 2.01$.

As has been pointed out [10], in order to obtain all relevant parameters of the spin Hamiltonian of a solid sample, a full powder pattern HFEPR spectrum must be obtained. We have thus restrained the polycrystalline Mn(salen) in a KBr pellet, or alternatively in *n*-eicosane mull. Spectra of the KBr pellet are shown in Fig. 6a at 193 GHz, and Fig. 6d at 289 GHz. It is obvious that these are low-quality spectra, with true spectral turning points hidden under the features that are artifacts due to

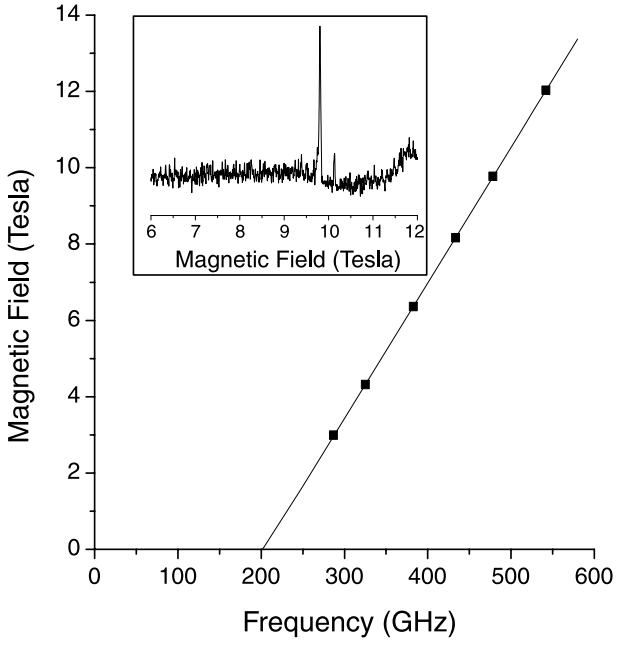

Fig. 5. HFEPR spectrum of loose polycrystalline Mn(salen) at 478.5 GHz and $T = 5.0$ K (inset), and the resonance field vs. frequency of the signal observed at this temperature (main plot). The squares are experimental points while the straight line was drawn using best-fitted spin Hamiltonian parameters: $D = -2.24\,\mathrm{cm}^{-1}$, $E = 0$, and $g_z = 2.01$.

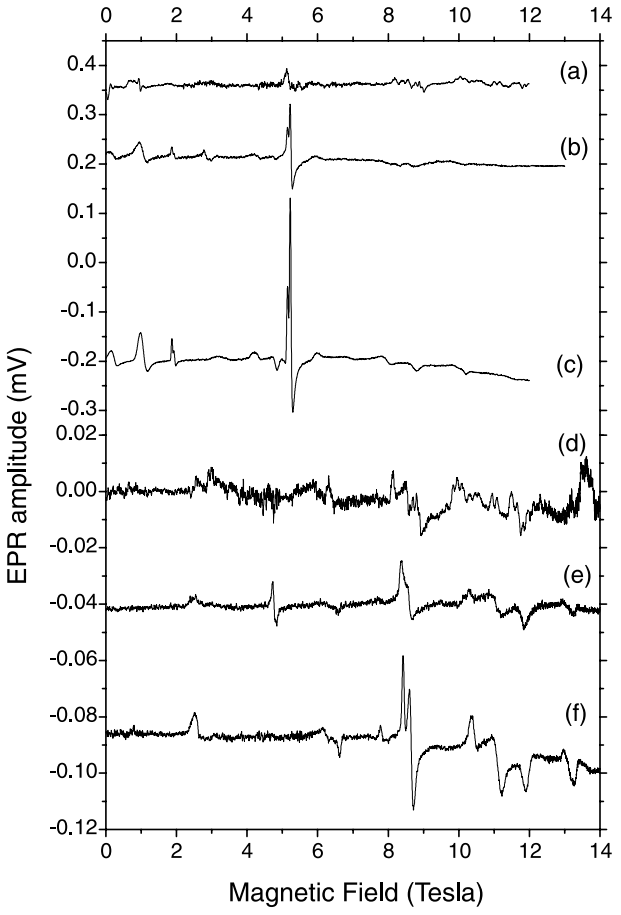

Fig. 6. (a) Experimental HFEPR spectrum of Mn(salen) pressed into a KBr pellet at 192.8 GHz and $T = 30$ K recorded in the transmission-type spectrometer; (b) spectrum of a solution in neat CH_2Cl_2 at 30 K; (c) spectrum in a CH_2Cl_2:toluene 3:2 v/v mixture; (d) spectrum of the same pellet as in (a) at 289.1 GHz; (e) spectrum of the same solution as in (b) at 288.9 GHz; (f) spectrum of the same solution as in (c) at 289.1 GHz. The amount of Mn(salen) was the same (35 mg) in all experiments. All other experimental parameters are as in Fig. 1.

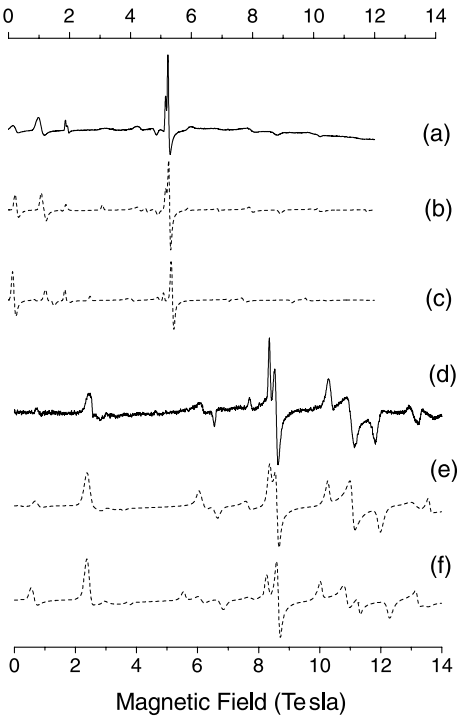

Fig. 7. (a) Experimental HFEPR spectrum of Mn(salen) in a CH_2Cl_2:toluene 3:2 v/v mixture at 192.7 GHz and $T = 30$ K; (b) simulation at the same frequency and temperature using $D = -2.47\,cm^{-1}$, $|E| = 0.17\,cm^{-1}$, $g(iso) = 2.00$; single-crystal linewidths 50 mT (parallel) and 30 mT (perpendicular); (c) simulation at the same frequency and temperature using $D = -2.50\,cm^{-1}$, $|E| = 0.27\,cm^{-1}$, $g_{x,y} = 2.00$; $g_z = 1.98$; (d) experimental spectrum at 289.1 GHz and $T = 30$ K; (e) simulation at the same frequency and temperature using $D = -2.47\,cm^{-1}$, $|E| = 0.17\,cm^{-1}$, $g(iso) = 2.00$, single-crystal linewidth as in (b); (f) simulation at the same frequency and temperature using $D = -2.50\,cm^{-1}$, $|E| = 0.27\,cm^{-1}$, $g_{x,y} = 2.00$; $g_z = 1.98$. Experimental parameters as in Fig. 1.

incomplete randomization of the sample, and incomplete restraint on pellet surfaces. Similar low-quality spectra were obtained from *n*-eicosane mulls.

HFEPR spectra of Mn(salen) in frozen organic solution (neat CH_2Cl_2) on the other hand, were of high quality (Fig. 6b at 193 GHz and Fig. 6e at 289 GHz). One can see a significant improvement in S/N ratio over the pellet spectrum, and disappearance of artifacts. The S/N ratio and the resolution of particular spectral features could be further significantly improved by preparing a mixed solvent glass, using CH_2Cl_2:toluene (3:2 v/v mixture; see Fig. 6c at 193 GHz, and Fig. 6f at 289 GHz). Note that in all six experiments presented in Fig. 6, the Mn(salen) amount (35 mg) was kept constant to facilitate comparison of the S/N achieved in different conditions. Despite improved resolution in the CH_2Cl_2:toluene glass, no hyperfine structure due to nuclear $I = 5/2$ spin of ^{55}Mn was observed even after diluting the solution to the limit of detection.

In order to determine accurately the spin Hamiltonian parameters of Mn(salen) in frozen solution, simulations

Table 1
Spin Hamiltonian parameters of the Mn(III) complexes under study

Complex	D (cm^{-1})	$\|E\|$ (cm^{-1})	g(iso)
Mn(TSP) (solid)	−3.12(2)	0.00(1)	2.00(2)
Mn(TSP) (solution)	−3.16(2)	0.00(1)	2.00(2)
Mn(salen) (solid)	−2.24(3)	—	2.01(2)
Mn(salen) (solution)	−2.47(2)	0.17(1)	2.00(2)

were performed at several frequencies, and compared with experimental data. Fig. 7a shows an experimental spectrum recorded at 193 GHz, which is compared with a best-fit simulation (Fig. 7b) using spin Hamiltonian parameters as in Table 1, but also with a simulation using parameters obtained from a parallel-mode X-band experiment (Fig. 7c) [25]. Fig. 7d shows an experimental spectrum at 289 GHz, compared with simulations (Figs. 7e and f) using the same parameters as Figs. 7b and c, respectively. The best-fit spin Hamiltonian parameters are given in Table 1.

4. Discussion

4.1. Qualitative and quantitative considerations of frozen solution studies

A visual inspection of Fig. 6 shows that frozen solution spectra of Mn(salen) are superior to those of a KBr pellet in terms of (a) S/N ratio and (b) resolution. Both improvements can be safely attributed to the much better randomization of molecules provided by a frozen solution. Apparently, despite grinding and restraining the polycrystallites in the solid samples, such a randomization was not achieved in a pellet, nor *n*-eicosane mull. The better S/N ratio for the solutions can also be attributed to a reduction in absorption of millimeter- and sub-millimeter wave radiation by the solvent in comparison with the solid KBr medium or *n*-eicosane mull, and thus more available detected power. With regard to the solvent, it is evident that a binary solvent including toluene is a better medium for Mn(salen) than neat methylene chloride. This has been proven to be the case also for other Mn(III) complexes such as [Mn(OEP)Cl] (OEP = 2,3,7,8,12,13,17,18-octaethylporphyrinato) [29], or [Mn(TPP)Cl] [30]. It is known from both low-frequency EPR and optical studies that binary solvents often offer better glass quality than neat ones. Apparently the same is true for HFEPR.

It is interesting to observe that even for solid complexes that do *not* undergo torquing effects in magnetic field, such as Mn(TSP), there is an improvement of S/N ratio for the same sample amount in a frozen aqueous solution compared to neat solid sample (Fig. 1). This may have to do with better millimeter and sub-millimeter wave propagation properties of frozen solvents in general compared to the solid. Also, we observed that ice causes the smallest dielectric losses of all the frozen solvents we have tried in the frequency range of interest (95–380 GHz).

It has to be mentioned that when choosing the proper glass for a given complex, one has to bear in mind a possible chemical interaction between the solvent molecules and the complex under study, such as coordination. Thus for Mn(cor) (cor = 8,12-diethyl-2,3,7,13,17,18-hexamethylcorrolato) [11] dissolving the solid complex in pyridine caused a noticeable change in HFEPR spectra, attributed to axial coordination of pyridine via its nitrogen lone electron pair to the manganese ion. Analogously, a dissolution of [Mn(TPP)Cl] in the binary solvent used in this study, 3:2 v/v CH_2Cl_2:toluene brought about slight changes in HFEPR spectra [30]. In this case, although we could not obtain high-quality spectra of powdered solid Mn(salen), we could fairly accurately compare the spin Hamiltonian parameters of the complex isolated in glass with those of the solid. HFEPR experiment on the field-oriented solid sample (Fig. 5) points to a magnitude of $|D| = 2.24\,\mathrm{cm}^{-1}$ in a solid, which is about 10% lower than that in the glass. This is much more than the 1% uncertainty associated with our procedure of obtaining D through a linear fit to the parallel $|2,-2\rangle \rightarrow |2,-1\rangle$ transition, and is thus meaningful. As for the water-soluble Mn(TSP) complex, the zfs parameter measured for the solid sample ($D = -3.12\,\mathrm{cm}^{-1}$) differs from the one measured in solution ($D = -3.16\,\mathrm{cm}^{-1}$) only minimally, since the difference between the two is just outside the experimental error. The values for E and g remain unchanged. The D value determined for Mn(TSP) has significantly larger magnitude than found in a variety of porphyrinic complexes of Mn(III) [9–11,29,30], in particular Mn(TPP)Cl, for which $D = -2.29\,\mathrm{cm}^{-1}$ in a solid, [10], and $-2.50\,\mathrm{cm}^{-1}$ in frozen solution [30]. An analysis of the electronic structural implications of this finding is beyond the scope of this paper. We note that dissolving Mn(TSP) in water does not change its spin Hamiltonian parameters within experimental error, so that water is an 'innocent' solvent for this particular complex, while for Mn(salen), the organic solvent causes an increase in the magnitude of $|D|$ by about 10%.

In summary of the solid vs. glass comparison, it can be stated that for the several Mn(III) complexes measured by HFEPR so far, frozen solution provides a much better randomization of the molecules, and thus improves the quality of the spectra both in terms of S/N ratio and resolution. The limiting factor here is the solubility of the given complex, since concentration sensitivity requirements of HFEPR instrumentation (see below) require a range of concentrations that is relatively high compared to other techniques. Some high-spin complexes of transition metal ions cannot thus be measured in frozen solution due to limited solubility in all 'innocent' solvents known.

4.2. Comparison of HFEPR with parallel-mode X-band EPR

An $S = 2$ spin system is not always 'EPR-silent' even in the case of large zfs parameters. As shown in Fig. 4, a rhombic parameter E mixes the wavefunctions corresponding to the two lowest spin sublevels designated $|2^a\rangle$

and $|2^s\rangle$, causing those two levels to split with the energy difference equal to $\Delta = 3E^2/D$. In many cases, this value is on the order of the X-band EPR energy quantum ($\sim 0.3\,\mathrm{cm}^{-1}$). Since mixing the wavefunctions also makes the transition between them partly allowed, an X-band EPR signal can often be observed at very low fields in a $S = 2$ spin system such as Fe(II) [34]. The intensity of this transition can be significantly increased by use of parallel-mode detection [34]. This so-called "non-Kramers signal" was first observed in a Mn(III) complex a number of years ago [35], but only recently, Campbell et al. [25,28] analyzed such signals quantitatively. In particular, they extracted spin Hamiltonian parameters for the complex of our interest, reporting for Mn(salen) in CH_2Cl_2 with added NMO: $D = -2.50\,\mathrm{cm}^{-1}$, $|E| = 0.269\,\mathrm{cm}^{-1}$, $g_x = g_y = 2.00$; $g_z = 1.98$, and for Mn(salen) with added 4-PPNO (4-phenylpyridine-*N*-oxide), the same parameters except $|E| = 0.249\,\mathrm{cm}^{-1}$ [25]. Without these additives, which are weakly coordinating, parallel-mode X-band EPR of Mn(salen) in CH_2Cl_2 solution shows multiple spin species, whose natures are not clear. The presence of well-resolved hyperfine structure due to ^{55}Mn (100%, $I = 5/2$) was of particular help in spectral analysis.

HFEPR showed no evidence for multiple spin species for Mn(salen) in CH_2Cl_2/toluene (3:2 v/v) solution. A clear powder pattern spectrum was observed corresponding to a single spin species, characterized by the following spin Hamiltonian parameters: $D = -2.47\,\mathrm{cm}^{-1}$, $|E| = 0.17\,\mathrm{cm}^{-1}$, $g(\mathrm{iso}) = 2.00$. Adding NMO did not change the HFEPR spectra in any visible way. We have simulated the HFEPR spectra obtained at two frequencies: 193 and 289 GHz using two sets of spin Hamiltonian parameters: the best-fit set as above, and one corresponding to the values of Campbell et al. (Fig. 7) [25]. One can see that while the value of D is essentially confirmed since our result is within experimental error identical to that of Campbell et al., our $|E|$ is about 40% smaller than theirs. HFEPR is superior to X-band detection in the number of transitions observable. The accuracy of spin Hamiltonian parameters obtained by HFEPR is correspondingly higher than that achieved by X-band EPR. In particular, the splitting observed in the HFEPR signal at 5.2 T at 193 GHz, and 8.4 T at 289 GHz is directly proportional to $|E|$. We have tried to simulate our experimental spectra using parameters of Campbell et al. (Figs. 7c and f). It is clear that the agreement between the experiment and simulation in such a case is much poorer than with the parameters listed in Table 1. This is due to a different value of $|E|$, which can be determined directly from HFEPR spectra. One reason for the differences between our parameters, and those obtained by Campbell et al. may be due to differences in composition of the low-temperature glass. Campbell used neat CH_2Cl_2, while we used a CH_2Cl_2/toluene (3:2 v/v) solution, which vastly improved spectral quality (Fig. 6). It is possible that the binary solvent eliminates some of the multiple species visible in the X-band spectra by improving glass quality, so that only one species is clearly visible in our HFEPR spectra. Campbell et al. [25] also observed a spectral change upon addition of NMO to Mn(salen) in neat CH_2Cl_2, but we saw no such effect of NMO in the mixed CH_2Cl_2/toluene glass. Toluene is a weak Lewis donor, so it may be competing with NMO in coordinating the manganese ion. The reasons for possible chemical differences between our HFEPR, and Campbell's X-band results remain outside the scope of the present paper, but need to be investigated in more depth further, as they may be of relevance to the catalytic behavior of the complex [24,25]. We note here simply that, although there is significant variation in ligand among salen (N_2O_2 donor), tetrapyrroles such as TPP (N_4 donors), and Me_2dbm (O_4 donor; Me_2dbm^- is the anion of 4,4′-dimethyldibenzoylmethane) [29], all of these square pyramidal Mn(III) complexes with axial chloro ligands give axial zfs in the range $-2.35 < D < -2.55\,\mathrm{cm}^{-1}$.

It is not clear, however, whether the differences in the spin Hamiltonian parameters of Mn(salen) obtained by HFEPR, and X-band are indeed of chemical origin. It was observed very early on by Gerritsen and Sabisky [41] for the Mn^{3+} ion in a rutile crystal, that the zero-field energy difference between the $|2^a\rangle$ and $|2^s\rangle$ levels depends not only on D and E through the term $\Delta = 3E^2/D$, but also on the cubic fourth-order Hamiltonian term, a [3] (see Fig. 4). In the case of a comparable to E, as in their system, the zero-field energy gap may be predominantly determined by a rather than Δ. A non-negligible a value thus affects the field position of the X-band signal since the latter depends directly on the zero-field energy gap between the $|2^a\rangle$ and $|2^s\rangle$ levels. Computer simulations indicate that introduction of an a term of the magnitude observed by Gerritsen and Sabisky [41], $|a| \approx 0.1\,\mathrm{cm}^{-1}$, combined with the HFEPR value, $|E| = 0.17\,\mathrm{cm}^{-1}$, yields a good agreement with the X-band signal observed by Campbell et al. [25]. At the same time, this magnitude of a shifts simulated HFEPR lines only within the observed linewidths. Based on the results presented and discussed above, it appears that proper spectral analysis including higher-order spin Hamiltonian terms can be achieved in the case of solution spectra only by combining both techniques. As we discuss elsewhere [45], while HFEPR is superior in the sense that it can unequivocally and accurately determine the $\boldsymbol{g}$ tensor, and second-order zfs terms, X-band EPR is more sensitive to the fourth-order terms, notably cubic term a, due to generally smaller linewidths. It should be noted that HFEPR as performed on single crystals can also very accurately determine fourth-order spin Hamiltonian terms [46]. It is also evident, as witnessed by the failure to record X-band spectra for Mn(TSP), that low-frequency EPR does not work for systems characterized by a strictly axial zfs tensor, such as porphyrinic complexes of Mn(III), since in such

conditions the $|2,-2\rangle \rightarrow |2,+2\rangle$ transition becomes strictly forbidden, and these systems are truly 'EPR-silent' at low frequency/field conditions.

A clear superiority of parallel-mode X-band EPR in comparison with HFEPR lies in the potential of observing hyperfine structure, which in the case of Campbell et al. [25] was very helpful in determining the existence of multiple spin species in the sample. Despite many attempts on solutions of Mn(salen) and Mn(TPP) in organic solutions, and Mn(TSP) in aqueous media, we have failed to observe hfs on any HFEPR line, and tend to believe that it may not be feasible in general. We have eliminated the most obvious reason for line broadening, namely that originating from spin–spin interactions of the dipolar/exchange type, which are normally responsible for obscuring hfs in neat solid complexes, by diluting the solutions to the detection limit. Among the many other possible reasons for the broadening effect that obscures hfs in high frequency/field conditions, strain effects occurring in glasses are the most probable cause [47]. Rather than attempting to differentiate among the at least three possible strain phenomena affecting the relevant spin Hamiltonian parameters of a high-spin system: zfs parameters [48], hfs constants [49], and g-factors [50], we make a comparison to the Mn(II) ion ($3d^5, S = 5/2$), which is characterized by the same nuclear spin, $I = 5/2$, and generally an almost isotropic g tensor, as in Mn(III). It is well established that EPR spectra of Mn(II) actually profit from high frequency/field conditions in terms of reduced linewidth due to a decrease in the significance of high-order spin Hamiltonian terms relative to the Zeeman energy [51]. Hfs is thus readily detected in Mn(II) complexes by HFEPR, and we observed it in the Mn(II) impurity which commonly appears in solution HFEPR spectra of Mn(III). However, there are marked differences between the $S = 5/2$ Mn(II), and the $S = 2$ Mn(III) ions. The spectral improvement as frequency is increased [51] is generally the case for Mn(II) complexes with relatively small zfs, such as $[Mn(H_2O)_6]^{2+}$, for which $|D| < 0.03\,cm^{-1}$. For this species, $|D|$ becomes much smaller than the microwave quantum at frequencies above X-band, which causes a reduction of second-order effects originating from zfs and affecting the linewidth, and consequently a reduction of observed linewidth. In the Mn(III) complexes studied here, the zfs magnitudes are much larger, on the order of 2.4–3.2 cm^{-1}, which means we never reach true high-frequency conditions, and thus the effect described above may not be operational. For Mn(II) complexes of low symmetry, such as those observed in metalloproteins, in which D is often quite large, hfs is usually observed in HFEPR spectra only within the central Kramers signal corresponding to the $|5/2,-1/2\rangle \rightarrow |5/2,+1/2\rangle$ transition, while in all other fine structure transitions it is effectively smeared out. Higher frequency reduces the intensities of forbidden transitions of the type $|5/2,-1/2,M_I\rangle \rightarrow |5/2,+1/2,M_I+1\rangle$, thus sharpening/increasing the intensities of the allowed $|5/2,-1/2,\ M_I\rangle \rightarrow |5/2,+1/2,M_I\rangle$ transitions, which are insensitive to the effects of D-strain. The other allowed transitions, e.g., $|5/2,-5/2,M_I\rangle \rightarrow |5/2,-3/2,M_I\rangle$ are very sensitive to D-strain, which far overwhelms the benefits afforded by higher frequency in terms of hyperfine transitions. A significant broadening occurs on all of these fine structure transitions of the $S = 5/2$ spin system, so that they appear only as a broad background under the central line [52]. Since an $S = 2$ spin system has no equivalent to the $|5/2,-1/2\rangle \rightarrow |5/2,+1/2\rangle$ transition characteristic for the Kramers ion Mn(II), which is free of D-strain effects, we do not expect to observe hfs on any transition for Mn(III) in high frequency/field conditions even in dilute solutions, unless of course the Mn(III) is in a high symmetry site.

4.3. Concentration sensitivity of HFEPR instruments

It has been early on recognized [1], that concentration sensitivity of current HFEPR instrumentation may be the limiting factor in applying this technique to transition metal ion research, particularly metalloproteins. To understand it better, it is necessary to distinguish *absolute* sensitivity from *concentration* sensitivity. The former is defined [53] as the minimum *number* of unpaired electron spins detectable by an EPR instrument with a 1:1 S/N ratio, usually in conditions normalized to 1 Gauss linewidth, and 1 Hz bandwidth. The concentration sensitivity is defined [1] as a minimum *concentration* of the given spin species detectable by an instrument with a 1:1 S/N ratio. The concentration sensitivity of current HFEPR spectrometers is generally poorer than that of conventional X-band machines principally due to either of two instrumental factors: (a) a much smaller sample volume in spectrometers equipped with a resonator, or (b) a much lower B_1 field in instruments operating without a cavity. As an instrument-independent factor, the increased spectral dispersion characteristic for high frequency and field conditions generally causes a lowering of signal amplitude for the same sample in comparison with conventional EPR. Since no numerical values for minimal concentration sensitivity have been reported to our best knowledge, we have estimated the concentration sensitivity of both HFEPR instruments used in this study, extrapolating the achieved S/N ratio to 1:1. The values obtained this way in the transmission HFEPR spectrometer are collected in Table 2. They indicate that this type of HFEPR spectrometer can measure aqueous solution samples with concentrations in the 100 μM range using the second harmonic of the Gunn source, which cor-

Table 2
S/N ratios of frozen solution HFEPR spectra of Mn(III) complexes under study in the transmission-type spectrometer

Complex	Solvent	Concentration (mM)	S/N ratio at 190 GHz	S/N ratio at 285 GHz	Concentration sensitivity at 190 GHz (μM)	Concentration sensitivity at 285 GHz (mM)
Mn(TSP)	Water	55	500:1	65:1	110	0.86
Mn(salen)	CH_2Cl_2:toluene	220	250:1	35:1	900	6
[Mn(TPP)Cl]	CH_2Cl_2:toluene	230	440:1	16:1	500	14

responds to the frequency range of 185–225 GHz and in the 1 mM range using the third harmonic of this source, which corresponds to the frequency range of 275–335 GHz. For Mn(III) complexes soluble only in organic glasses, the same values are 0.5–1.0 mM for the second harmonic, and 6–15 mM for the third harmonic. The new-generation reflection-type quasi-optical spectrometer improves (lowers) these values by a factor of 3–4, although it does offer an improved *absolute* sensitivity by a factor of 20–40 (C. Saylor et al., to be published).

The question arises whether the above values are of general meaning, or specific to the complexes studied. We believe they should hold at least for high-spin Mn(III) ($S = 2$) complexes as long as their characteristic relaxation rates do not change drastically, since the overall sensitivity depends on the spin relaxation properties [54]. This is particularly valid for metalloproteins, which in general are fast-relaxing due to the numerous, low energy vibrational modes in these large molecules, which can couple to electronic spin levels [55]. The influence of varying relaxation rates on the concentration sensitivity can be only speculated for species not yet successfully detected in solution, such as Fe(II).

5. Conclusions

The principal aim of this work was a systematic analysis of the problems encountered while employing HFEPR to study high-spin non-Kramers ions in frozen solutions, using two high-spin ($S = 2$) Mn(III) complexes as test cases. The complexes, Mn(TSP) and Mn(salen), are respectively an axial spin system soluble in aqueous solution and a (slightly) rhombic spin system soluble in organic solvents (here, neat CH_2Cl_2 and CH_2Cl_2/toluene 3:2 (v/v)). We have demonstrated that high-quality HFEPR spectra can be recorded for these complexes in both frozen aqueous ($S/N = 500{:}1$ at 55 mM) and organic solvents ($S/N = 250{:}1$ at 220 mM) and that very precise ($\pm 0.02\,\mathrm{cm}^{-1}$) zfs parameters can be readily determined from multifrequency spectra.

A secondary objective was a comparison of the two alternative EPR techniques used to study $S = 2$ transition metal complexes in frozen solution: HFEPR versus parallel-mode X-band EPR. We show that the accuracy of the zfs parameters, particularly the rhombic term, $|E|$, is much higher when obtained from HFEPR than that obtainable from a single-frequency (typically X-band) parallel mode "non-Kramers" signal. Equally important, for $S = 2$ systems with $E = 0$ (rigorously axial systems, such as typical Mn(III) porphyrins), parallel mode provides no advantage over conventional X-band EPR and the systems are "EPR-silent." Neither does HFEPR require the presence of state-mixing caused by rhombic splitting, as numerous allowed EPR transitions inaccessible at low fields and frequencies are directly observed. On the other hand, X-band EPR, characterized by a smaller linewidth, allowed us to estimate the cubic fourth-order zfs term a, which is hidden under increased HFEPR linewidths. Since X-band EPR allows also to observe hfs in Mn(III), which is not amenable to HFEPR detection in solutions, it is preferable to use both techniques in studying $S = 2$ species.

Finally, we estimated the concentration sensitivities of two HFEPR spectrometers used in this study. We found an improvement by employing quasi-optical architecture and homodyne design by a factor of 3–4 over the transmission-type apparatus. Such an improvement, however small, may be sufficient for the study of metalloproteins [1], wherein a concentration of > 10 mM, such as used here for small molecules, might not be feasible, but a concentration of $\leqslant 10$ mM can well be. Further development of millimeter and sub-millimeter wave technology will certainly improve these parameters.

Acknowledgments

We thank Dr. H. Weihe (Ørsted Institute, Copenhagen, Denmark), for providing us with the simulation package SIM, and for very helpful discussions, and Mr. Greg Yeagle and Prof. R. David Britt (UC-Davis) for performing the parallel-mode X-band EPR experiment on Mn(TSP). Dr. C. Saylor's implementation of the quasi-optical homodyne HFEPR spectrometer is appreciated, as are helpful discussions with Dr. L.-C. Brunel. We thank the NHMFL (In-House Research

Grant to J.K., visitor subsidy to J.T.) and Roosevelt University (J.T.) for support.

References

[1] W. Hagen, High-frequency EPR of transition ion complexes and metalloproteins, Coord. Chem. Rev. 190 (1999) 209–229.

[2] A.-L. Barra, L.-C. Brunel, D. Gatteschi, L. Pardi, R. Sessoli, High-frequency EPR spectroscopy of large metal ion clusters: from zero field splitting to quantum tunneling of magnetization, Acc. Chem. Res. 31 (1998) 460–466.

[3] A. Abragam, B. Bleaney, Electron Paramagnetic Resonance of Transition Ions, Dover Publications Inc., New York, 1986.

[4] J. Telser, L.A. Pardi, J. Krzystek, L.-C. Brunel, EPR spectra from 'EPR-silent' species: high-field EPR spectroscopy of aqueous chromium(II), Inorg. Chem. 37 (1998) 5769–5775.

[5] M.J. Knapp, J. Krzystek, L.-C. Brunel, D.N. Hendrickson, High-frequency EPR study of the ferrous ion in the reduced rubredoxin model $[Fe(SPh)_4]^{2-}$, Inorg. Chem. 39 (2000) 281–288.

[6] P.L.W. Tregenna-Piggott, H. Weihe, J. Bendix, A.-L. Barra, H.-U. Güdel, High-field, multifrequency EPR study of the vanadium(III) hexaaqua cation, Inorg. Chem. 38 (1999) 5928–5929.

[7] D. Collison, M. Helliwell, V.M. Jones, F.E. Mabbs, A.J.L. McInnes, P.C. Riedi, G.M. Smith, R.G. Pritchard, W.I. Cross, Single and double quantum transitions in the multi-frequency continuous wave electron paramagnetic resonance (cwEPR) of three six-coordinate nickel(II) complexes: $[Ni(EtL)_2(Me_5dien)]$ and $[Ni(5\text{-methylpyrazole})_6]X_2$, $X = (ClO_4)^-$ or $(BF_4)^-$. The single crystal X-ray structure at room temperature of $[Ni(5\text{-methylpyrazole})_6](ClO_4)_2$, J. Chem. Soc., Faraday Trans. 94 (1998) 3019–3025.

[8] A.-L. Barra, D. Gatteschi, R. Sessoli, G.L. Abbati, A. Cornia, A.C. Fabretti, M.G. Uytterhoeven, Electronic structure of manganese(III) compounds from high-frequency EPR spectra, Angew. Chem. Intl. Ed. Engl. 36 (1997) 2329–2331.

[9] D.P. Goldberg, J. Telser, J. Krzystek, A.G. Montalban, L.-C. Brunel, A.G.M. Barrett, B.M. Hoffman, EPR spectra from "EPR-silent" species: high-field EPR spectroscopy of manganese(III) porphyrins, J. Am. Chem. Soc. 119 (1997) 8722–8723.

[10] J. Krzystek, J. Telser, L.A. Pardi, D.P. Goldberg, B.M. Hoffman, L.-C. Brunel, High-frequency and -field electron paramagnetic resonance of high-spin manganese(III) in porphyrinic compelxes, Inorg. Chem. 38 (1999) 6121–6129.

[11] J. Krzystek, J. Telser, B.M. Hoffman, L.-C. Brunel, S. Licoccia, High-frequency and field EPR investigation of (8,12-diethyl-2,3,7,13,18-hexamethylcorrolato)manganese(III), J. Am. Chem. Soc. 123 (2001) 7890–7897.

[12] J. Bendix, H.B. Gray, G. Golubkhov, Z. Gross, High-field (high-frequency) EPR spectroscopy and structural characterization of a novel manganese(III) corrole, J. Chem. Soc., Chem. Commun. (2000) 1957–1958.

[13] J. Limburg, J.S. Vrettos, R.H. Crabtree, G.W. Brudvig, J.C. de Paula, A. Hassan, A.-L. Barra, C. Duboc-Toia, M.-N. Collomb, High-frequency EPR study of a new mononuclear manganese(III) complex: $[(terpy)Mn(N_3)_3]$ (terpy = 2,2′:6′,2-terpyridine), Inorg. Chem. 40 (2001) 1698–1703.

[14] G. Aromi, J.P. Claude, M.J. Knapp, J.C. Huffman, D.N. Hendrickson, G. Christou, High-spin molecules: hexanuclear $[Mn_6O_4Cl_4(Me_2dbm)_6]$ (Me_2 dbmh = 4,4′-dimethyldibenzoylmethane) with a near tetrahedral $[Mn_6O_4Cl_4]^{6+}$ core and a $S = 12$ ground state, J. Am. Chem. Soc. 120 (1998) 2977–2978.

[15] G. Aromi, M.J. Knapp, J.P. Claude, J.C. Huffman, D.N. Hendrickson, G. Christou, High-spin molecules: hexanuclear Mn(III) clusters with $[Mn_6O_4X_4]^{6+}$ ($X = Cl^-, Br^-$) face-capped octahedral cores and $S = 12$ ground states, J. Am. Chem. Soc. 121 (1999) 5489–5499.

[16] P. Artus, C. Boskovic, J. Yoo, W.E. Streib, L.-C. Brunel, D.N. Hendrickson, G. Christou, Single-molecule magnets: site-specific ligand abstraction from $[Mn_{12}O_{12}(O_2CR)_{16}(H_2O)_4]$ and the preparation and properties of $[Mn_{12}O_{12}(NO_3)_4(O_2CCH_2Bu^t)_{12}(H_2O)_4]$, Inorg. Chem. 40 (2001) 4199–4210.

[17] J. Yoo, A. Yamaguchi, M. Nakano, J. Krzystek, W.E. Streib, L.-C. Brunel, H. Ishimoto, G. Christou, D.N. Hendrickson, Mixed-valence tetranuclear manganese single-molecule magnets, Inorg. Chem. 40 (2001) 4604–4616.

[18] A. Caneschi, D. Gatteschi, R. Sessoli, A.L. Barra, L.C. Brunel, M. Guillot, Alternating current susceptibility, high field magnetization, and millimeter band EPR evidence for a ground $S = 10$ state in $[Mn_{12}O_{12}(CH_3COO)_{16}(H_2O)_4] \cdot 2CH_3COOH \cdot 4H_2O$, J. Am. Chem. Soc. 113 (1991) 5873–5874.

[19] A.L. Barra, A. Caneschi, D. Gatteschi, R. Sessoli, High-frequency EPR spectra for the analysis of magnetic anisotropy in large magnetic clusters, J. Am. Chem. Soc. 117 (1995) 8855–8856.

[20] J.S. Miller, C. Vazquez, J.C. Calabrese, R.S. McLean, A.J. Epstein, Cooperative magnetic behavior of α- and β-manganese (III) phthalocyanine tetracyanoethenide (1:1), (MnPc)(TCNE), Adv. Mater. 6 (1994) 217–221.

[21] J.S. Miller, J.C. Calabrese, R.S. McLean, A.J. Epstein, *Meso*-(tetraphenylporphinato)manganese(III)-tetracyanoethenide, $(MnTPP)^+ (TCNE)^-$. A new structure-type linear-chain magnet with a T_c of 18 K, Adv. Mater. 4 (1992) 498–501.

[22] J.S. Miller, C. Vazquez, N.L. Jones, R.S. McLean, A.J. Epstein, Magnetic behavior of octaethylporphinatomanganese(III) tetracyanoethenide, [MnOEP][TCNE], and hexacyanobutadienide, $[MnOEP][C_4(CN)_6]$. The importance of a unifrom chain for stabilizing strong effective ferromagnetic coupling, J. Mater. Chem. 5 (1995) 707–711.

[23] R.A. Sheldon (Ed.), Metalloporphyrins in Catalytic Oxidations, Marcel Dekker, New York, 1994.

[24] E.N. Jacobsen, M.H. Wu, in: E.N. Jacobsen, A. Pfaltz, H. Yamamoto (Eds.), Comprehensive Asymmetric Synthesis, Springer, New York, 1999, pp. 649–677.

[25] K.A. Campbell, M.R. Lashley, J.K. Wyatt, M.H. Nantz, R.D. Britt, Dual-mode EPR study of Mn(III) salen and the Mn(III) salen-catalyzed epoxidation of *cis*-β-methylstyrene, J. Am. Chem. Soc. 123 (2001) 5710–5719.

[26] I. Fridovich, Superoxide radical and superoxide dismutases, Annu. Rev. Biochem. 64 (1995) 97–112, and references therein.

[27] K.M. Faulkner, S.I. Liochev, I. Fridovich, Stable Mn(III) porphyrins mimic superoxide dismutase in vitro and substitute for it in vivo, J. Biol. Chem. 269 (1994) 23471–23476.

[28] K.A. Campbell, E. Yikilmaz, C.V. Grant, W. Gregor, A.-F. Miller, R.D. Britt, Parallel polarization EPR characterization of the Mn(III) center of oxidized manganese superoxide dismutase, J. Am. Chem. Soc. 121 (1999) 4714–4715.

[29] J. Krzystek, J. Telser, M.J. Knapp, D.N. Hendrickson, G. Aromi, G. Christou, A. Angerhofer, L.-C. Brunel, High-frequency and -field electron paramagnetic resonance of high-spin manganese(III) in axially symmetric coordination complexes, Appl. Magn. Reson. 23 (2001) 571–585.

[30] J. Krzystek, L.A. Pardi, L.-C. Brunel, D.P. Goldberg, B.M. Hoffman, S. Licoccia, J. Telser, High-frequency and -field electron paramagnetic resonance of high-spin manganese(III) in tetrapyrrole complexes, Spectrochim. Acta, Part A 58 (2002) 1113–1127.

[31] This complex is more correctly [Mn(TSP)Cl] in the solid state, however, we do not know the axial ligand(s) in aqueous solution and refer to all forms of the complex simply as Mn(TSP).

[32] The name salen is normally applied to bis(salicylidene)-1,2-ethanediamine, rather than a 1,2-cyclohexanediamine compound,

such as Jacobsen's catalyst. However, for consistency with the earlier study [25] we refer here to Jacobsen's catalyst as Mn(salen). The nature of the axial ligand(s) in this complex in solution (Cl in the solid state) is likewise not certain.

[33] J. Hanson, Synthesis and use of Jacobsen's catalyst: enantioselective epoxidation in the introductory organic laboratory, J. Chem. Educ. 78 (2001) 1266–1268.

[34] M. Hendrich, P. Debrunner, Integer-spin electron paramagnetic resonance of iron proteins, Biophys. J. 56 (1989) 489–506.

[35] S.L. Dexheimer, J.W. Gohdes, M.K. Chan, K.S. Hagen, W.H. Armstrong, M.P. Klein, Detection of EPR spectra in $S = 2$ states of trivalent manganese complexes, J. Am. Chem. Soc. 111 (1989) 8923–8925.

[36] A.K. Hassan, L.A. Pardi, J. Krzystek, A. Sienkiewicz, P. Goy, M. Rohrer, L.-C. Brunel, Ultrawide band multifrequency high-field EMR technique: a methodology for increasing spectroscopic information, J. Magn. Reson. 142 (2000) 300–312.

[37] G.M. Smith, J.C.G. Lesurf, R.H. Mitchell, P.C. Riedi, A high performance mm-wave electron spin resonance spectrometer, IEEE MTT-S Digest (1995) 1677–1680.

[38] G.M. Smith, J.C.G. Lesurf, R.H. Mitchell, P.C. Riedi, Quasi-optical cw mm-wave electron spin resonance spectrometer, Rev. Sci. Instrum. 69 (1998) 3924–3937.

[39] C.J.H. Jacobsen, E. Pedersen, J. Villadsen, H. Weihe, ESR characterization of *trans*-$V^{II}(py)_4X_2$ and *trans*-$Mn^{II}(py)_4X_2$ (X = NCS, Cl, Br, I; py = pyridine), Inorg. Chem. 32 (1993) 1216–1221.

[40] Simulation software is available from Dr. H. Weihe; for more information see the www page: <http://sophus.kiku.dk/software/epr/epr.html>.

[41] H.J. Gerritsen, E.S. Sabisky, Paramagnetic resonance of trivalent manganese in rutile (TiO_2), Phys. Rev. 132 (1963) 1507–1512.

[42] J. Krzystek, J.-H. Park, M.W. Meisel, M.A. Hitchman, H. Stratemeier, L.-C. Brunel, J. Telser, EPR spectra from EPR-silent species: high-frequency and -field EPR spectroscopy of pseudo-tetrahedral complexes of nickel(II), Inorg. Chem. 41 (2002) 4478–4487.

[43] L.A. Pardi, A.K. Hassan, F.B. Hulsbergen, J. Reedijk, A.L. Spek, L.-C. Brunel, Direct determination of the single-ion anisotropy in a one-dimensional magnetic system by high-field EPR spectroscopy; synthesis, EPR, and X-ray structure of $Ni_xZn_{1-x}(C_2O_4)(dmiz)_2$ [$x = 0.07$], Inorg. Chem. 39 (2000) 159–164.

[44] Mn(III) corrole complexes, which lack the four-fold symmetry of porphyrins, do exhibit non-zero E [11,12].

[45] J. Krzystek, G. Yeagle, J.-H. Park, M.W. Meisel, R.D. Britt, L.-C. Brunel, J. Telser, High frequency and field EPR spectroscopy of tris(2,4-pentanedionato)manganese(III): investigation of solid-state versus solution Jahn–Teller effects, Inorg. Chem. (submitted).

[46] S. Mossin, M. Stefan, P. ter Heerdt, A. Bouwen, E. Goovaerts, H. Weihe, Fourth-order zero-field splitting parameters of [Mn(cyclam)Br_2]Br determined by single crystal W-band EPR, Appl. Magn. Reson. 21 (2002) 586.

[47] D. Mustafi, E.V. Galtseva, J. Krzystek, L.C. Brunel, M.W. Makinen, High-frequency electron paramagnetic resonance studies of VO^{2+} in low-temperature glasses, J. Phys. Chem. A 103 (1999) 11279–11286.

[48] B.J. Gaffney, B.C. Maguire, R.T. Weber, G.G. Maresch, Disorder at metal sites in proteins: a high-frequency-EMR study, Appl. Magn. Reson. 16 (1999) 206–221.

[49] W. Froncisz, J.S. Hyde, Broadening by strains of lines in the g-parallel region of Cu^{2+} EPR spectra, J. Chem. Phys. 73 (1980) 3123–3131.

[50] R.E. Anderson, W.R. Dunham, R.H. Sands, A.J. Bearden, H.L. Crespi, On the nature of the iron sulfur cluster in a deuterated algal ferredoxin, Biochim. Biophys. Acta 408 (1975) 306–318.

[51] B.F. Bellew, C.J. Halkides, G.J. Gerfen, R.G. Griffin, D.J. Singel, High frequency (139.5 GHz) electron paramagnetic resonance characterization of Mn(II)–$H_2{}^{17}O$ interactions in GDP and GTP forms of p21 ras, Biochemistry 35 (1996) 12186–12193.

[52] P. Manikandan, R. Carmieli, T. Shane, A.J. Kalb, D. Goldfarb, W-band ENDOR investigation of the manganese-binding site of concanavalin A: determination of proton hyperfine couplings and their signs, J. Am. Chem. Soc. 122 (2000) 3488–3494.

[53] C.P. Poole, Electron Spin Resonance, Dover Publications Inc., Mineola, 1983.

[54] T.D. Smith, J.R. Pilbrow (Eds.), ESR of Iron Proteins, Plenum Press, New York, 1980.

[55] S.S. Eaton, G.R. Eaton (Eds.), Relaxation Times of Organic Radicals and Transition Metal Ions, Kluwer, New York, 2000.